Reply to Reviewer #1 Comments

General comment

Present work is a case study of a possible interaction of atmospheric gravity waves (GWs) and equatorial plasma bubbles (EPBs). The authors observed South to North propagation of GWs, when an EPB was drifting eastward. After the interaction, the EPB (DP1) revived, extending its latitudinal extension and the 6300 depletion became much stronger. The authors tried to explain the observational evidence as an interaction of E-field generated by GWs and EPB. They concluded that "fossil depletion" DP1 revived and became an "active depletion" under the passage of GWs." The interpretation and argument are interesting and worth to pointing and to discuss, since such observational reports are still limited in the literature.

Reply: We sincerely thank the esteemed Reviewer for his tremendous encouragement and invaluable insight into our submission. His critical comments have provided us with insightful perspectives to enhance the clarity and robustness of our findings. We have tried our level best to address his concerns in this Revised Version.

However, I feel a serious concern in the airglow images and the image data analysis. Regarding the signature of thermospheric gravity waves (f1, f2), the authors mentioned that the wave crests can be seen clearly in Figure 1 and Figure 3(c,d). To my seeing, it is very difficult to recognize the wave fronts f1 and f2 from Figure 1 and 3(c, d). Since the wave fronts in question are located close to the image horizon, it is further difficult to resolve horizontal structure. The authors should explain how they transferred the images in geographic coordinates and calculate the wave characteristics. If it is not the case, how the linear coordinates are decided. Besides it, the optical filter for 6300 imaging normally includes OH emissions, of which intensity is much stronger near the horizon, say 75 to 80 degree of zenith angle. How the authors could eliminate the OH contamination. The authors can explain those mattes in the section of Instrumentation and data analysis procedure.

Reply: Sincere thanks for these critical comments and suggestions which indeed helped us to improve the presentation of our results.

1. We agree with Reviewer that the signatures of thermospheric gravity waves are not clear and very faint. Under these situations, time-difference (TD) images have proven ability to reflect the faint GWs activity. We generated such TD images and present below some of them during 1742-1830 UT that do show faint fronts of GWs. We present labelled and unlabelled sequence of OI 630 nm images, respectively, on the left and right for the kind preview of Reviewer.
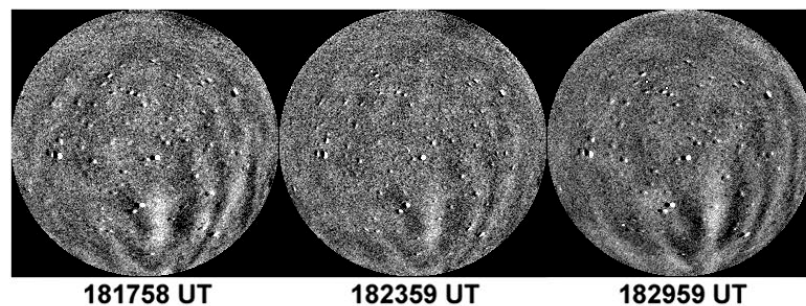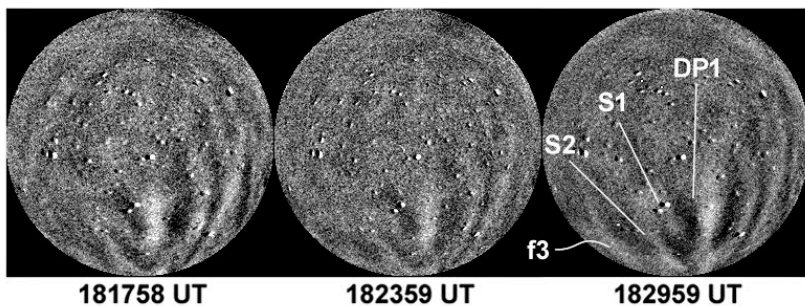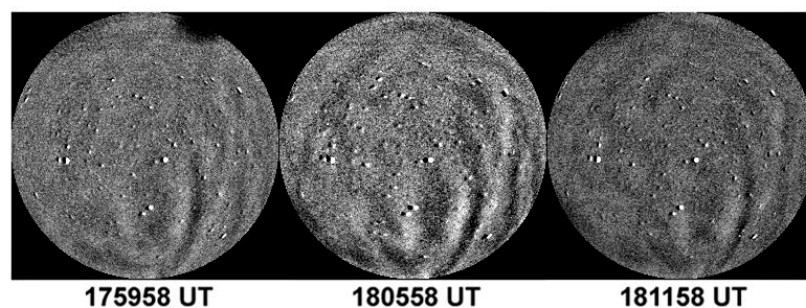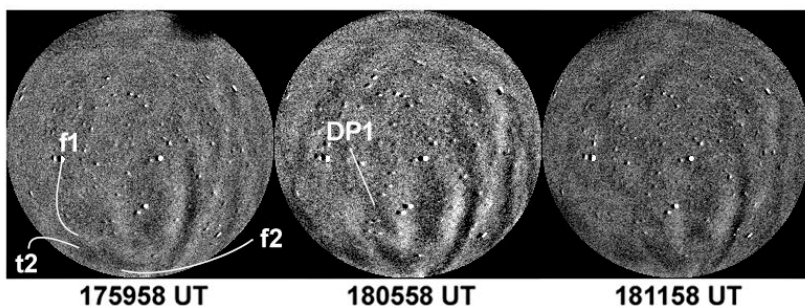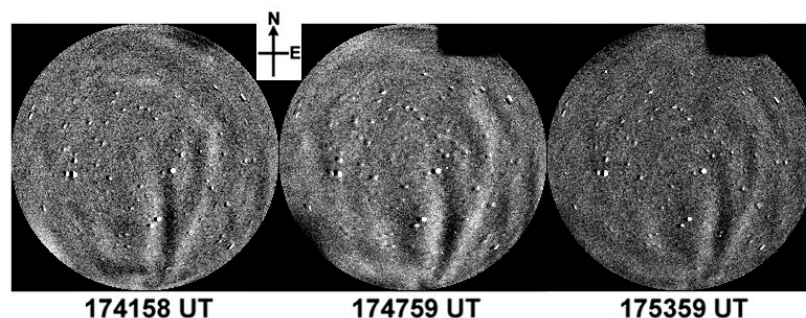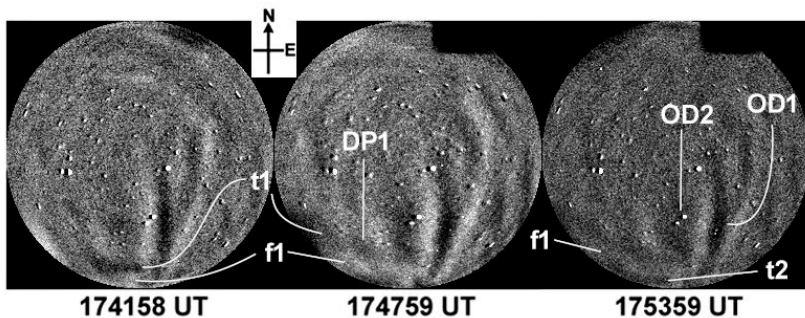
2. As suggested, we have Re-written the **Introduction and data** section as under as:

Under the *CAWSES India Phase II Programme*, an ASAI was installed for limited nightglow observations at Ranchi (23.3º N, 85.3º E, mlat. ~19º N), located near the crest of equatorial ionization anomaly (EIA) in India during April 2012. Parihar et al. (2017) and Parihar (2019) have described this ASAI system in detail. OI 630 nm emission was monitored using a 2.2 nm half-power bandwidth optical filter having transmittance of ~77%. Our imager's field-of-view roughly covered about 7-8° latitude/longitude region at 250 km over Ranchi. Airglow images were flat-fielded to reduce the inhomogeneous contribution at lower elevations due to van Rhijn effect and non-uniform sensitivity of CCD detector at different pixels. Next, following the technique described by Wrasse et al. (2021), we detrended the individual images to enhance the contrast of airglow features using an hour running average image. Using known astral positions and assuming OI 630 nm emission peak at 250 km, the geographic coordinates of each pixel was determined following the technique of Garcia et al. (1997). Using this information, all-sky images were unwarped. We follow the technique discussed by Pimenta et al. (2003) to determine the drift velocity of depletions. First, for a given latitude, two intensity profiles along east-west direction as a function of distance was generated using two successive unwarped images. Next, the east-west displacement of depletion was estimated using these two profiles from which drift speed was determined (see Pimenta et al., 2003 for details of this technique). Similarly, the propagation characteristics of GW fronts were estimated by tracking faint crest and trough along the propagation direction in the consecutive images. As GW fronts were unclear in images, we used contrast-enhanced images. We, also, generated NS keograms to visualize GW traces and determine their speed. A keogram is a time-versus-latitude plot generated by extracting a NS column from individual images and stacking them horizontally. Next, GWs speed was, also, estimated from the slope of wave traces seen in these keograms (Makela et al., 2006). We looked into the total electron content (TEC) measurements from an *International GNSS Service* station Hyderabad (17.3° N, 78.6° E, mlat. ~12.0° N, located nearby and south of Ranchi) to ascertain GW activity seen in the ASAI observations (Source: https://t-ict4d.ictp.it/nequick2/gnss-tec-calibration, Ciraolo et al., 2007). Quiet geomagnetic conditions prevailed on this night with *Kp < 2, Ap = 4,* and *– 4 < Dst < 10 nT*.

3. We describe in brief the technique used by Pimenta et al. (2003) to estimate the drift velocity of depletions and GWs.

Using known astral positions and assuming OI 630 nm emission peak at 250 km, the geographic coordinates of each pixel was determined following the technique of Garcia et al. (1997). Using this information, all-sky images were unwarped. We follow the technique discussed by Pimenta et al. (2003) to determine the drift velocity of depletions. First, for a given latitude, two intensity profiles along east-west direction as a function of distance was generated using two successive unwarped images. Next, the east-west displacement of depletion was estimated using these two profiles from which drift speed was determined (see Pimenta et al., 2003 for details of this technique). Similarly, the propagation characteristics of GW fronts were estimated by tracking faint crest and trough along the propagation direction in the consecutive images. As GW fronts were unclear in images, we used contrast-enhanced images. We, also, generated NS keograms to visualize GW traces and determine their speed.

A typical unwarped image at 192358 UT in presented below:
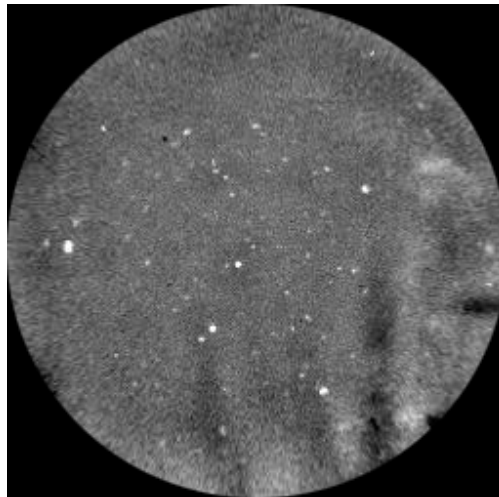
4. We agree with Reviewer that OH emissions can contaminate OI 630 nm nightglow. We used a 2.2 nm narrow half-power bandwidth optical filter to monitor OI 630 nm emission which can be contaminated by P_2 line of OH (9, 3) Meinel band at 629.8 nm. As a cross-check, we looked into OH broadband emission which indicated no GW activity at the MLT region. A typical OH broadband image is presented below:

We, further, looked into TEC measurements from an IGS station Hyderabad (located nearby and south of Ranchi) which do show the presence of wave like variations. As such, we believe that GW fronts seen in OI 630 nm are the signatures of thermospheric GW activity.

In conclusion, the present manuscript would be necessary to improve data analysis method and to convince readers to see the clear signature of wave structure of GWs in the 6300 emission layer.

Reply: We sincerely thank Reviewer for this critical comment. We have tried to bring out clarity in Presentation and Figures to show the signatures of GWs in OI 630 nm images.

Individual comments are below:
Line 133 (filter characteristics of 6300 imaging): please include the filter characteristics (HPBW, for example).

Reply: Many thanks. We have added this information.
Correction: OI 630 nm emission was monitored using a 2.2 nm half-power bandwidth optical filter having transmittance of ~77%.

Line 144 (keogram): please mention how to produce the keogram and how to calculate the wave characteristics from the keogram. What is the latitudinal extension (in km) of the keogram Figure 3 (a, b) ?

Reply: Many thanks. We have added the following text in this Revised version.

Correction 1: A keogram is a time-versus-latitude plot generated by extracting a NS column from individual images and stacking them horizontally. Next, GWs speed was, also, estimated from the slope of wave traces seen in these keograms (Makela et al., 2006).

Correction 2: We have corrected the Figure for latitudinal extension as under as:
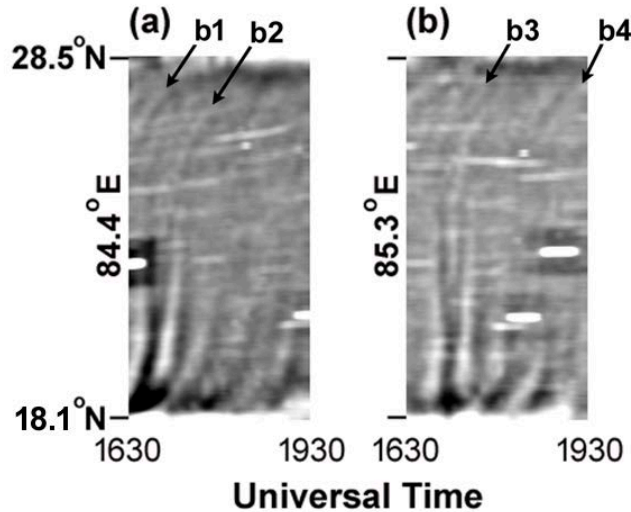
Line 161 (keogram): Are these keograms made by using original images or geographically coordinated (unwarped) images ? Please make indication by arrow the GW signature in the Figures 3 (a) and (b).

Reply: Many thanks. We have generated keograms from flat-fielded and contrast enhanced images. Used images were not geographically corrected ones. We have considered a NS column of individual images corresponding to desired longitude as depicted below and stacked them horizontally.
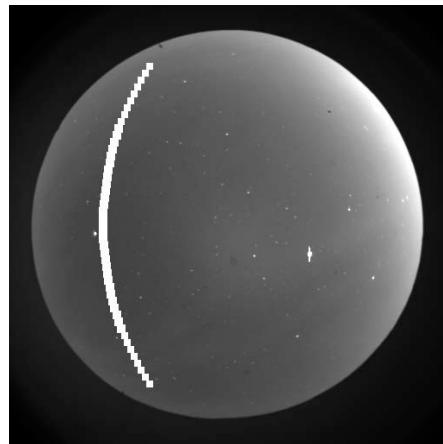
We have, also, marked the GW traces by black arrow 'b1', 'b2', 'b3' and 'b4' used for determining their phase speed as suggested.

Lines 166-167 (Being faint in nature, GWs signatures in ASAI images were getting lost in the geographic unwarping process): As the authors mentioned, it is difficult to estimate wave characteristics from the wave crests located at a large zenith angle. It means that there is a large uncertainty to get the wave characteristics from the wave fronts located in the corner of an all sky image. If the wave fronts (f1 and f2) are located at around 75 to 80 degrees of zenith angle, for example, one degree of distance corresponds to longer than 40-50 km at 250 km of altitude. The authors should keep in mind such uncertainty in their calculation of wave characteristics.

Reply: We agree with Reviewer and sincerely thank for this critical comment. We have considered the wave fronts and troughs located within 65 degrees of zenith angle. GW front 'f1' and trough preceding it were located within this range around 1800 UT. We have, also, relied on the wave traces seen over the North in NS keograms.

Line 169 (intensity profiling technique): Please explain the technique,

Reply: Many thanks. We have added the following text in "**Instrumentation and data**" Section:
Correction: We follow the technique discussed by Pimenta et al. (2003) to determine the drift velocity of depletions. First, for a given latitude, two intensity profiles along east-west direction as a function of distance was generated using two successive unwarped images. Next, the east-west displacement of depletion was estimated using these two profiles from which drift speed was determined (see Pimenta et al., 2003 for details of this technique). Similarly, the propagation characteristics of GW fronts were estimated by tracking faint crest and trough along the propagation direction in the consecutive images.

Line 170 (wave characteristics and Figure 3): The authors used keogramas (Figs 3(a,b) to calculate the wave characteristics. Please show explicitly the wave traces used in the figure. The authors pointed the wave signatures in the south edge of the image, However, the keograms show GW trace in the northern part. No propagating signature in the southern part. Please explain N-S scale of the keogram and put arrow signs to show the GW traces.

Reply: We sincerely thank with Reviewer and agree that wave traces were seen over North. Because of the co-existence of GW fronts and depletions together and their interaction over the South, we were unable to see such traces. As suggested, we have corrected the keograms as under as:
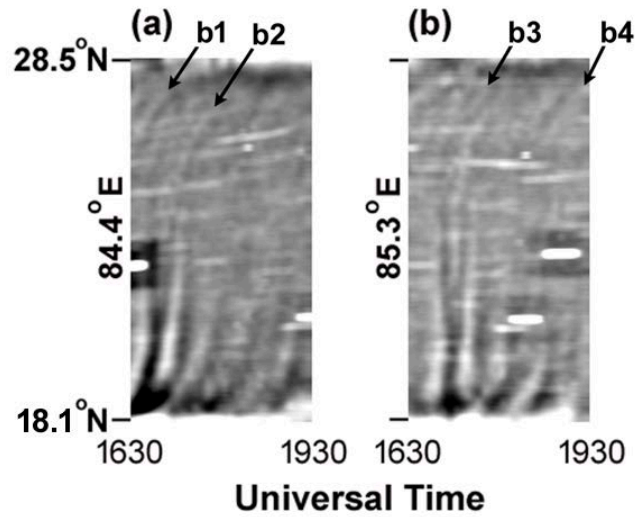
Line 176 (G27): Where is G27 ? Please point it.

Reply: Many thanks for pointing out this shortcoming in our presentation. We have limited the scatter plot to a few IPP trajectories and corrected Figure is as under as:
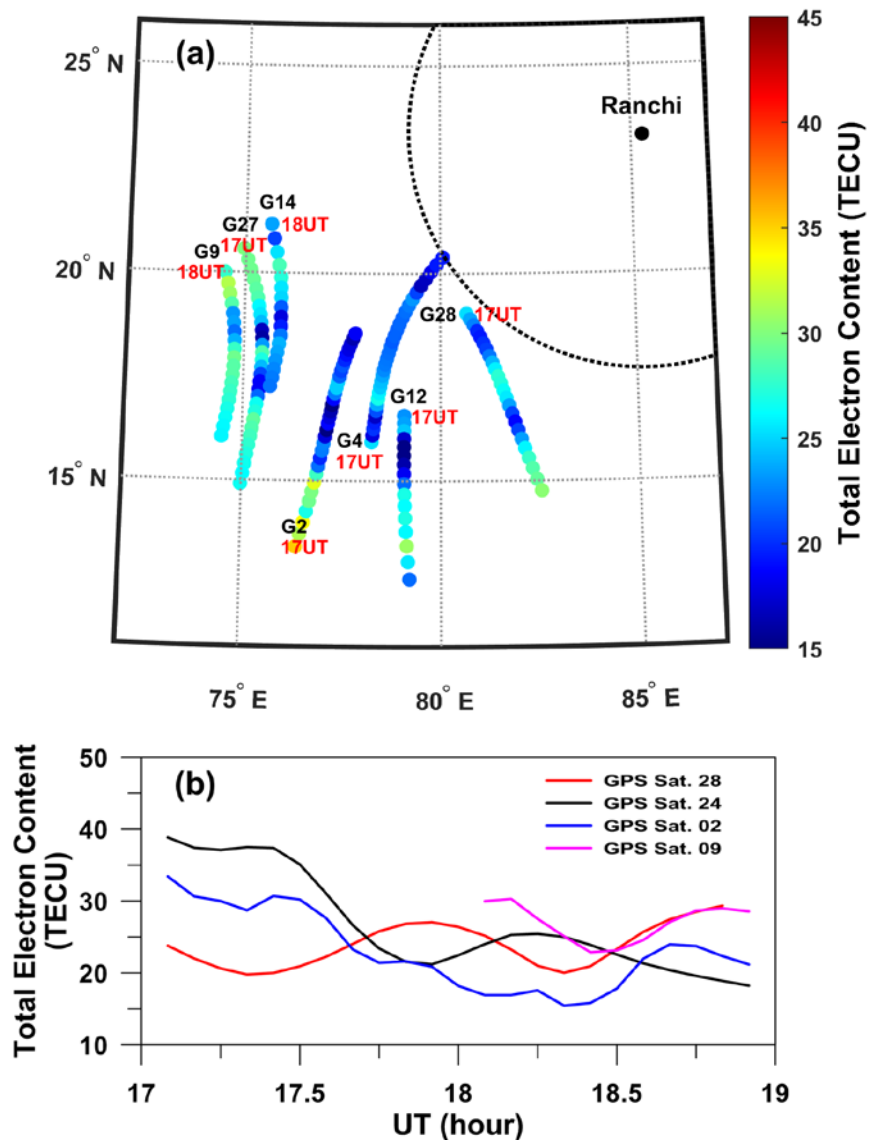
Line 180 (wave characteristics): please explain how the authors obtained this characteristic. Please remember that an IPP trajectory has two variables, time and space. Figure 3(f), therefore, shows TEC variation as a function of time and coordinates.

Reply: We sincerely thank Reviewer for bringing out this shortcoming in our presentation. We have corrected the text as under as:

Correction:

Of our interest is G28's TEC measurement as its IPPs trajectory lay close to the imager's ROI1 during 1700-1800 UT which showed a strong signature of GWs. By performing the periodogram

analysis of the temporal and spatial variation of its TEC, we estimated the propagation characteristics of GW to be τ ~0.95 ± 0.03 h, λ ~229 ± 12 km, and υ ~67 ± 5 m/s, and is in good agreement with the ASAI observations. Further, the propagation direction of GWs seen in airglow imaging is in good agreement with these previous reports.

Lines 198-204 and Figure 1: The authors tried to show the interaction of DP1 and GW f1 and f2, using Figure 1. However, it is hard to see such spatial and temporal variations of DP1, f1 and f2, those pointed by the authors. If the authors believe that the process was really happening, they must show airglow images with much clear way, perhaps increasing image contrast by subtracting one image from the other as shown in Figure 3(c,d).

Reply: We sincerely thank Reviewer for bringing out this shortcoming in our presentation. We have corrected **Figure 1** as:
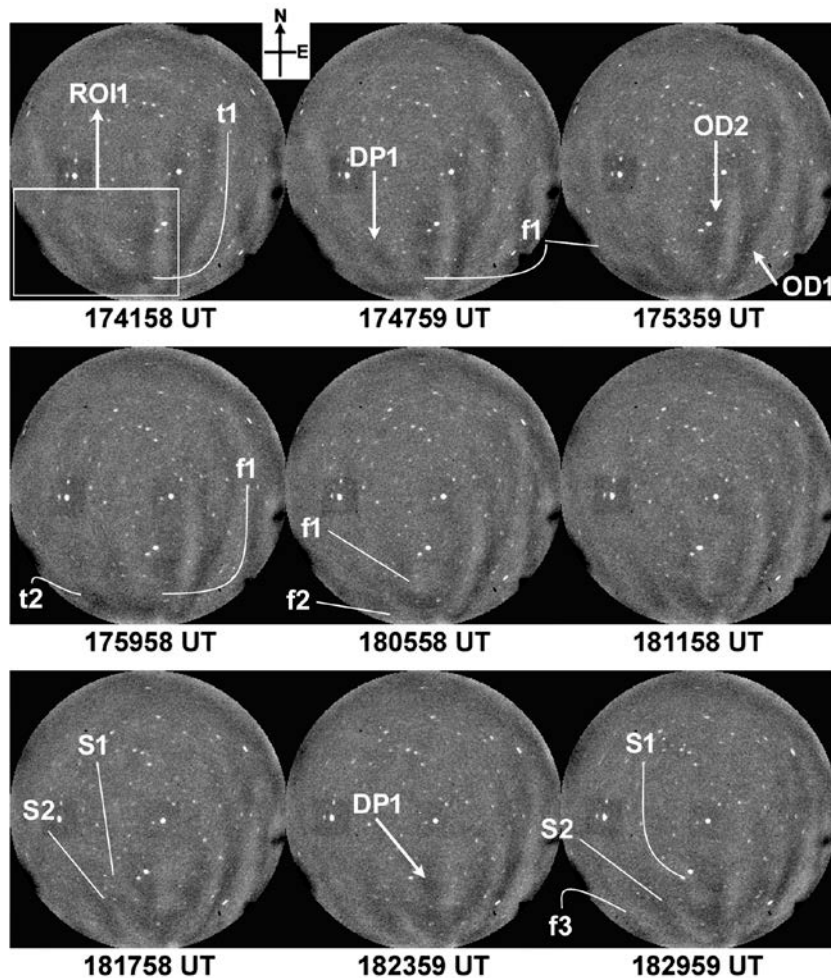
Corrected Figure 2:
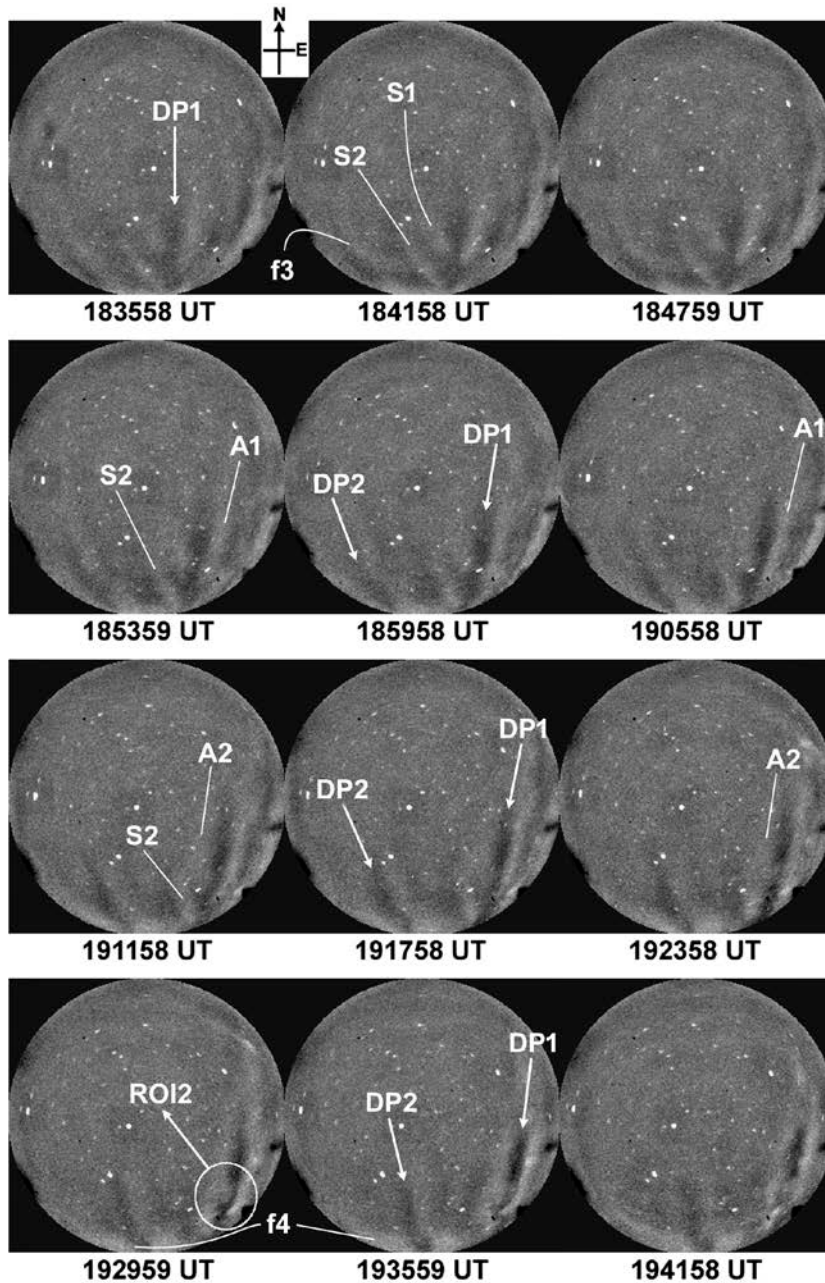
Lines 241-243 (GWs deform ,,,, act as a seed to GRT instability): please put references on it.

Reply: Many thanks. We have included References as under as:

Correction: GWs are well known to deform the bottom side plasma of the F-region into the wavelike ionization structures that then act as a seed to GRT instability, which, in turn, generates irregularities (Kelley et al., 1981; Hysell et al., 1990; Huba and Liu, 2020).

Reply to Reviewer #2 Comments

The manuscript "Simultaneous OI 630 nm imaging observations of thermospheric gravity waves and associated revival of fossil depletions around midnight near the EIA crest" by N. Parihar et al presents observations of airglow depletions from the low-to-mid-latitude station, Ranchi, India. The study focuses on the fossil depletions and their evolution in the presence of gravity waves. The main conclusion of the work is that the gravity waves can revive the observed fossil depletions. The presented observations and focus of the study are interesting and deserve publication. I am listing a few doubts which I encounter while reviewing the manuscript:

Reply: We sincerely thank the esteemed Reviewer for his tremendous encouragement and invaluable insight into our submission. His critical comments have provided us with insightful perspectives to enhance the clarity and robustness of our findings. We have tried our level best to address his concerns in this Revised Version.

(1) The airglow images are linearized or still suffer from the curvature effects?

Reply: Many thanks for this comment. During unwarping, faint features seen in all-sky images were getting lost. Hence, airglow images presented herein are not linearized and suffer from curvature effects. We used unwarped images to determine the eastward drift speed of depletions as well as the speed of GWs along the propagation direction.

(2) Authors should enlarge the ROI frame for clarity and to distinguish the gravity waves and depletions.

Reply: We sincerely thank Reviewer for this suggestion. We have added a New Figure of time difference images and Movie as Supplementary Material to show gravity waves. Probably because of their co-existence and interaction, GWs fronts and fossil depletion in early stage were not clearly seen in airglow images. Using the detrending technique suggested by Wrasse et al. (2021), we have prepared New Figure 1 and 2 as under as:

Corrected Figure 1:
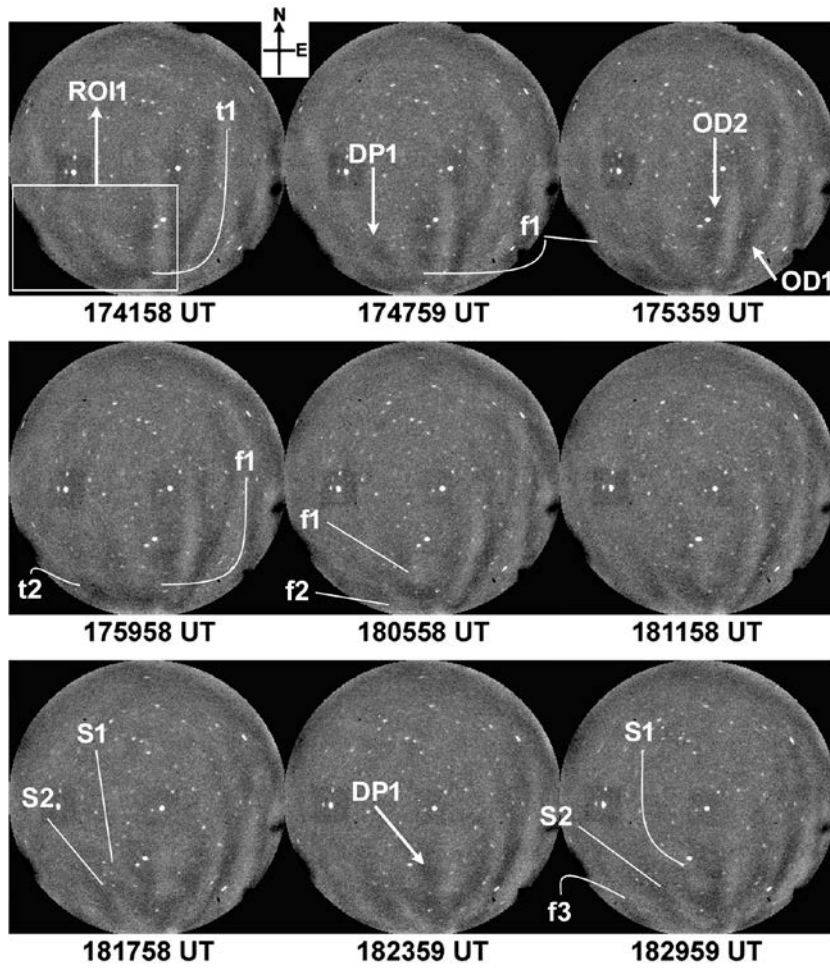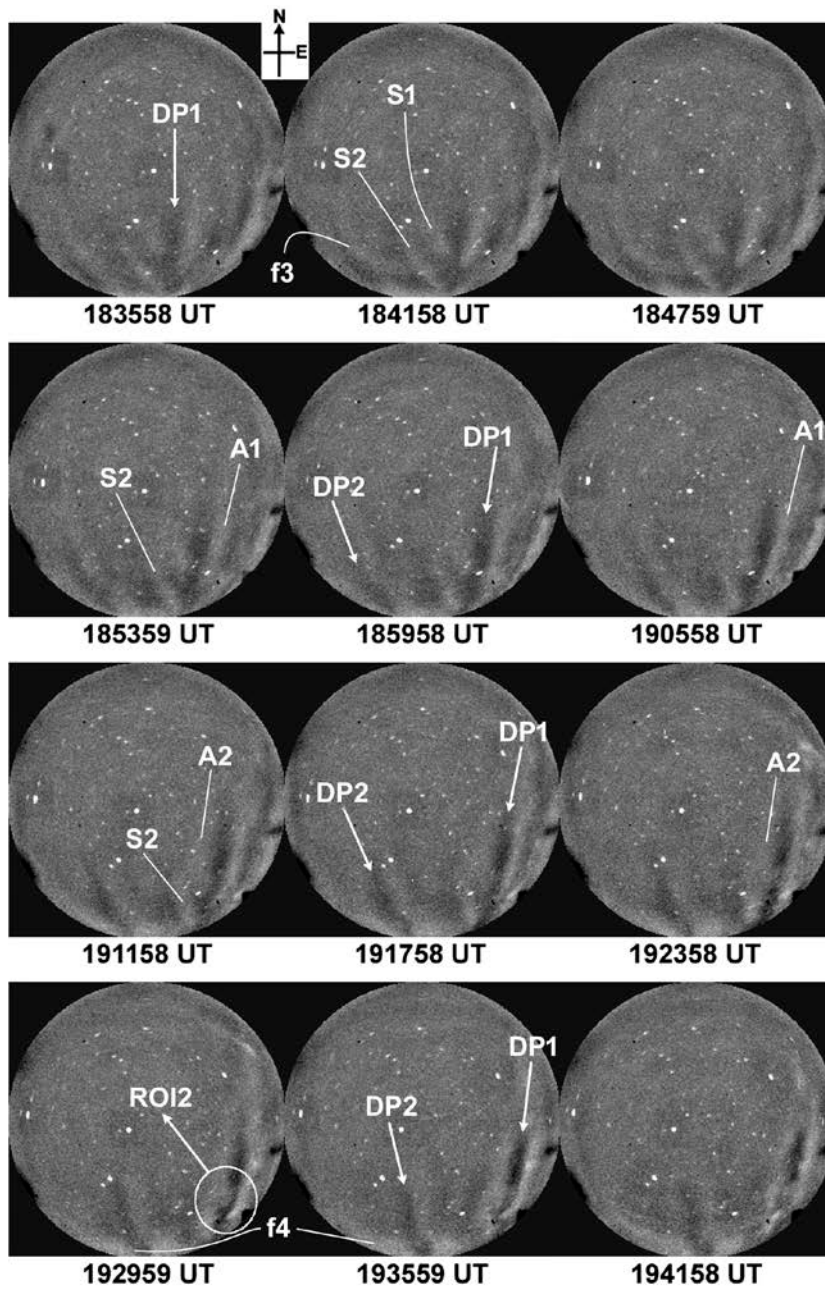
Corrected Figure 2:

New Figure 3: We generated such time difference images and present below some of them during 1742-1830 UT showing faint fronts of GWs. We present labelled and unlabelled sequence of OI 630 nm images, respectively, on the left and right for the kind preview of Reviewer.
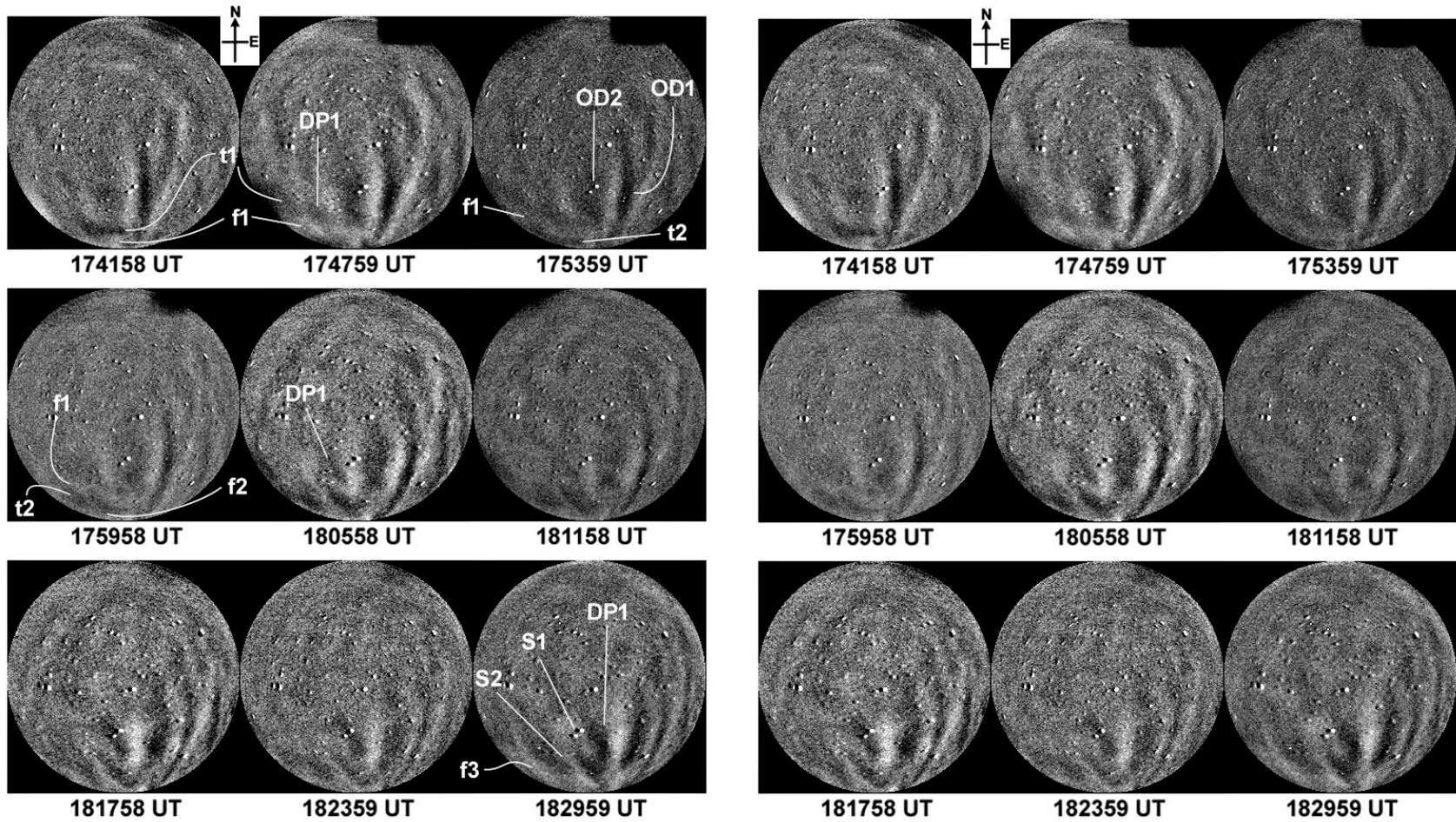
Correction in 'Observations' Section:

Supplementary material S1 shows the movie created from these images that feature this event.

(3) Should one refer to any dark patch at the corner of the airglow image as depletion?

Reply: Many thanks. We understand the concern of Reviewer. We were able to identify depletion after going through the sequence of images. We have included a Movie of all-sky images as Supplementary Material for the Preview of Reviewer.

(4) Both gravity waves and depletions characteristics are drawn from airglow observations. Does the author use any criteria to distinguish them?

Reply: Many thanks. We

(5) Obviously, if one draws their characteristics from the same image and the same region of interest, one would expect a kind of relationship that authors have found. To what extent this kind of approach is consistent and reasonable?

(6) Are the revivals of these fossil depletions are in-situ or the reflections of the equatorial energetics?

Reply: We sincerely thank the Reviewer for this critical comment. Using vertical TEC measurements from Hyderabad (17.3° N, 78.6° E, mlat. ~12.0° N, located nearby and south of Ranchi), we estimated the rate of change of TEC index (ROTI) and found ROTI index to increase from 17.25 to 20.25 during 1700-2000 UT. These ROTI values signify the presence of weak EPBs (Ma and Maruyama, 2006).

(7) If the revival is in-situ then why do authors discuss the apex height characteristics?

Reply: Many thanks. Because of complex interaction between GW fronts and depletions over the Southern edge of imaging, we were unable to determine the NS scale size of depletion DP1. Owing to this, we use Apex height to highlight the evolution of depletion DP1.

(8) If the revival is a reflection of the equatorial energetics then is it possible to have gravity waves reaching at 600 km altitude at the equator?

Reply: We sincerely thank the Reviewer for this critical comment and understand that this is not possible.

With these comments, I recommend the manuscript for publication with a minor revision.

Reply: We sincerely thanks Reviewer for this encouragement and critical comments which immensely helped us to improve our work.

Reply to Reviewer #3 Comments

The manuscript titled "Simultaneous OI 630 nm imaging observations of thermospheric gravity waves and associated revival of fossil depletions around midnight near the EIA crest" presents a possible interaction between thermospheric gravity waves (GWs) and fossil equatorial plasma bubbles (EPBs) over Ranchi, India, on 16 April 2012. The authors argue that after the interaction, the EPBs return to the growth stage.

However, the present manuscript contains some unclear data analysis and incomplete reasoning, which necessitates significant revision and clarification before it can be considered acceptable for publication. Only a few detailed comments are listed below.

Reply: We sincerely thank the esteemed Reviewer for his tremendous encouragement and invaluable insight into our submission. His critical comments have provided us with insightful perspectives to enhance the clarity and robustness of our findings. We have tried our level best to address his concerns in this Revised Version.

1. Regarding the new findings, the author claims to be the first to report the interaction between Gravity Waves (GW) and Equatorial Plasma Bubbles (EPBs) leading to latitudinal growth. However, Wrasse et al. (2021) (http://www.eppcgs.org//article/doi/10.26464/epp2021045?pageType=en) presented observational evidence of an interaction between EPBs and wave-like perturbations known as Medium-Scale Traveling Ionospheric Disturbances (MSTID) at low latitudes over the Brazilian sector. Wrasse et al. (2021) argued that electric fields associated with MSTID can intensify the growth of EPBs, leading to latitudinal and height expansion. Therefore, the authors should conduct an extensive bibliography review to properly address the novel findings presented in the study.

   Reply: We sincerely thanks Reviewer for this critical comment. We have included in this Revised Version the above-mentioned Reference as well as other similar works.

Correction:

In Introduction Section: Lately, Wrasse et al. (2021) presented an interesting event wherein a fossil EPB merged with other ones after interacting with an electrified MSTID and turned into an active bubble.

In Discussions Section: We know that the electric field perturbations associated with MSTIDs can influence the growth of irregularities. Otsuka et al. (2012) and Shiokawa et al. (2015) reported the disappearance of an EPB upon interaction with MSTIDs and large-scale traveling ionospheric disturbances (LSTIDs), respectively. Authors suggested that the electric field associated with MSTIDs/LSTIDs can move ambient plasma into the bubble across the geomagnetic field line through **E x B** drift which will result in the filling and subsequent disappearance of the depletion. Studies by Miller et al. (2009), Taori et al. (2015) and Takahashi et al. (2020) suggest that MSTIDs can directly seed EPBs. Simulation studies by Krall et al. (2011), further, indicates that the electric field associated with electrified MSTIDs can enhance the growth of EPBs. Lately, Wrasse et al. (2021) presented an interesting observations of the interaction of a fossil EPB with an electrified MSTID over 13.3° S. After interaction with the MSTID, concerned fossil EPB merged with other four EPBs, developed poleward and bifurcated. Using detrended TEC data, Takahashi et al. (2021) studied the large scale wave structures over Latin America and found them to be effective in seeding EPBs.

In References Section:

Wrasse, C. M., Figueiredo, C. A. O. B., Barros, D., Takahashi, H., Carrasco, A. J., Vital, L. F. R., Rezende, L. C. A., Egito, F., Rosa, G. M., and Sampaio, A. H. R.: Interaction between Equatorial Plasma Bubbles and a Medium-Scale Traveling Ionospheric Disturbance, observed by OI 630 nm airglow imaging at Bom Jesus de Lapa, Brazil. Earth Planet. Phys., 5(5), 397–406. https://doi.org/10.26464/epp2021045, 2021.

Takahashi, H., Wrasse, C. M., Figueiredo, C. A. O. B., Barros, D., Paulino, I., Essien, P., et al.: Equatorial plasma bubble occurrence under propagation of MSTID and MLT gravity waves. J. Geophys. Res.: Space Physics, 125, e2019JA027566. https://doi.org/10.1029/2019JA027566, 2020.

Takahashi, H., Essien, P., Figueiredo, C. A. O. B., Wrasse, C. M., Barros, D., Abdu, M. A., Otsuka, Y., Shiokawa, K., and Li, G. Z.: Multi-instrument study of longitudinal wave structures for plasma bubble seeding in the equatorial ionosphere. Earth Planet. Phys., 5(5), 368–377. https://doi.org/10.26464/epp2021047, 2021.

Krall, J., Huba, J. D., Ossakow, S. L., Joyce, G., Makela, J. J., Miller, E. S., and Kelley, M. C.: Modeling of equatorial plasma bubbles triggered by non-equatorial traveling ionospheric disturbances. Geophys. Res. Lett., 38(8), L08103. https://doi.org/10.1029/2011GL046890, 2011.

2. Regarding Figures 1 and 2, no clear signature of thermospheric gravity waves (GWs) can be observed in the OI 630 nm images. Additionally, there is no evident northward development visible in the equatorial plasma bubble (EPBs) structures. It is suggested that the authors include an OI 630 nm movie for the complete night of observation as "Supporting Information." This would enable a thorough assessment of the presence or absence of GWs, the evolution of EPBs, and the nature of their interaction throughout the observation period. Furthermore, the authors should consider employing alternative techniques to emphasize the interaction between GWs and EPBs, such as the detrended unwarped image technique demonstrated by Wrasse et al. (2021).

Reply: We sincerely thank the Reviewer for this critical comments and for suggesting us this crucial Reference on the detrending technique to improve our presentation. We have corrected Figure 1 and 2 following the technique described by Wrasse et al. (2021). We have, also, added a new figure (Figure 3) of time difference images that shows GW fronts. As suggested, we have added an OI 630 nm movie too.

Correction in 'Instrumentation and data' Section: Airglow images were flat-fielded to reduce the inhomogeneous contribution at lower elevations due to van Rhijn effect and non-uniform sensitivity of CCD detector at different pixels. Next, following the technique described by Wrasse et al. (2021), we detrended the individual images to enhance the contrast of airglow features using an hour running average image. Using known astral positions and assuming OI 630 nm emission peak at 250 km, the geographic coordinates of

each pixel was determined following the technique of Garcia et al. (1997). Using this information, all-sky images were unwarped.

Corrected Figure 1:
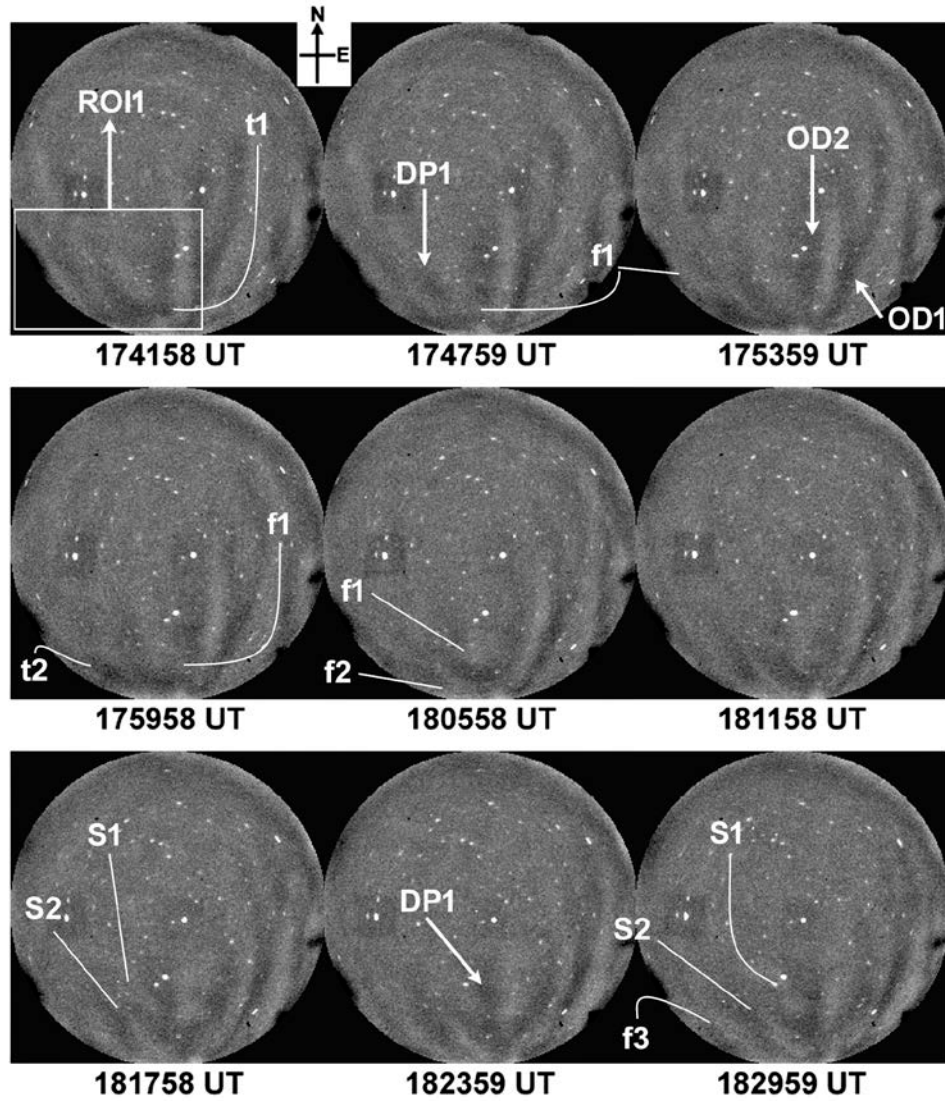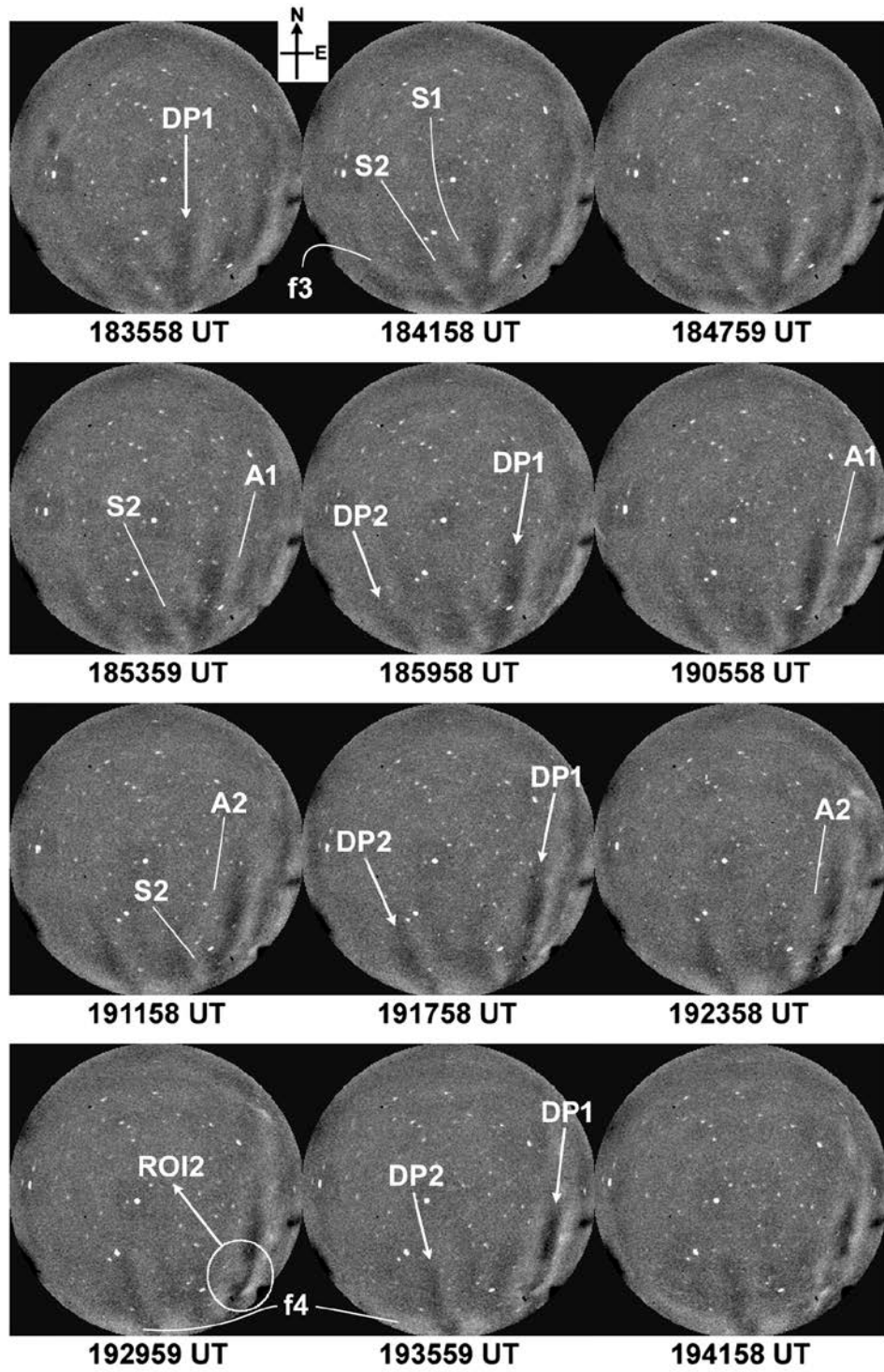
Corrected Figure 2:

New Figure 3: We generated such time difference images and present below some of them during 1742-1830 UT showing faint fronts of GWs. We present labelled and unlabelled sequence of OI 630 nm images, respectively, on the left and right for the kind preview of Reviewer.
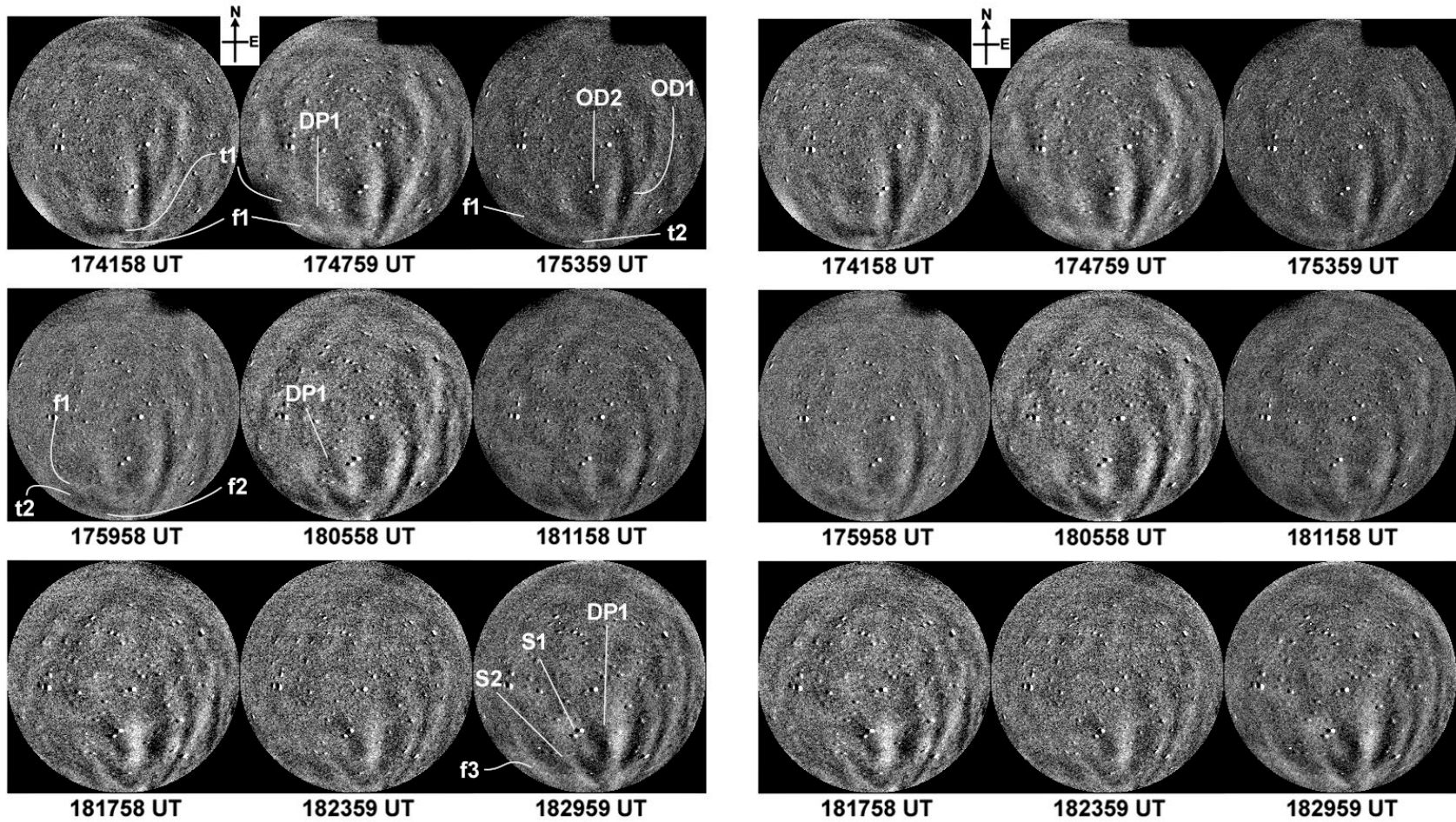
Correction in 'Observations' Section:

As the faint airglow features were getting lost in the unwarping process, warped all-sky images are presented. Supplementary material S1 shows the movie created from these images that feature this event.

3. The GWs signature in the TEC GPS IPP tracks are associated to a fluctuation of about 1-5% of the TEC level (e.g., Otsuka et al., 2013; Figueiredo et al., 2018; Takahashi et al., 2021/ https://angeo.copernicus.org/articles/31/163/2013/; https://agupubs.onlinelibrary.wiley.com/doi/full/10.1002/2017JA025021; http://www.eppcgs.org/en/article/doi/10.26464/epp2021047). Figure 3e and 3f present a TEC oscillation of about 10 TECU (see GPS PRN 28). This kind of TEC fluctuations are usually associated to EPBs signature (Barrros et al., 2018/https://angeo.copernicus.org/articles/36/91/2018/). Same interpretation can be done for Figure 3a and 3b, the north-south keograms clearly show EPBs signatures with their bifurcation. Therefore, the author should consider employing multiple GNSS receivers positioned near the event, or utilize various GNSS constellations (including GPS, GLONASS, Galileo, BeiDou), to accurately determine satellite IPP tracks corresponding to the same location as the OI 630 nm event. To achieve this, generating unwrapped images of OI 630 nm emissions is essential.

Reply: We sincerely thank the Reviewer for these critical References and suggestions on GNSS based analysis of this event. Presently, due to lack of expertise in GNSS data analysis, we are unable to address this comment of the reviewer. We indeed generated unwarped airglow images and a typical example at 192358 UT in presented below:
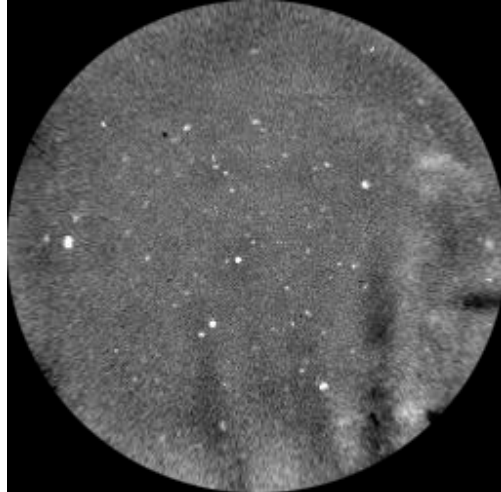
Regarding the bifurcations seen in NS keograms, we wish to state that these observed bifurcations are of a preceding depletion OD1 (shown in Figure 1).

4. The author should make an effort to present new analyses to thoroughly discuss the physical mechanisms underlying a possible revival of the EPBs. For instance, analysis of any enhancement of the polarization electric field inside the EPBs could be beneficial, with the assistance of ionosonde data collected near the event.

Reply: We greatly agree with these critical comments of Reviewer. Under *CAWSES India Phase II Programme*, Campaign-based Nightglow experiments were carried out at a temporary site Ranchi. Owing to this complementary experiments e.g. ionosonde and GPS were not available. Following this, we are unable to carry out the analysis suggested by Reviewer.